

PROCEEDINGS OF SPIE

SPIEDigitalLibrary.org/conference-proceedings-of-spie

Lidar-based detection and tracking of small UAVs

Marcus Hammer, Marcus Hebel, Martin Laurenzis,
Michael Arens

Marcus Hammer, Marcus Hebel, Martin Laurenzis, Michael Arens, "Lidar-based detection and tracking of small UAVs," Proc. SPIE 10799, Emerging Imaging and Sensing Technologies for Security and Defence III; and Unmanned Sensors, Systems, and Countermeasures, 107990S (4 October 2018); doi: 10.1117/12.2325702

SPIE.

Event: SPIE Security + Defence, 2018, Berlin, Germany

LiDAR-based detection and tracking of small UAVs

Marcus Hammer^{1a}, Marcus Hebel^a, Martin Laurenzis^b, Michael Arens^a

^aFraunhofer Institute of Optronics, System Technologies, and Image Exploitation IOSB,
Gutleuthausstr. 1, 76275 Ettlingen (Germany)

^bInstitut Franco-Allemand de Recherches de Saint-Louis, 5 Rue du Général Cassagnou, 68301 Saint-Louis (France)

ABSTRACT

The number of reported incidents caused by small UAVs, intentional as well as accidental, is rising. To avoid such incidents in future, it is essential to be able to detect UAVs. LiDAR sensors (e.g., laser scanners) are well known to be adequate sensors for object detection and tracking.

In this paper, we expand our existing LiDAR-based approach for the tracking and detection of (low) flying small objects like commercial mini/micro UAVs. We show that UAVs can be detected by the proposed methods, as long as the movements of the UAVs correspond to the LiDAR sensor's capabilities in scanning performance, range and resolution. The trajectory of the tracked object can further be analyzed to support the classification, meaning that UAVs and non-UAV objects can be distinguished by an identification of typical movement patterns. A stable tracking of the UAV is achieved by a precise prediction of its movement. In addition to this precise prediction of the target's position, the object detection, tracking and classification have to be achieved in real-time.

For the algorithm development and a performance analysis, we analyzed LiDAR data that we acquired during a field trial. Several different mini/micro UAVs were observed by a system of four 360° LiDAR sensors mounted to a car. Using this specific sensor system, the results show that UAVs can be detected and tracked by the proposed methods, allowing a protection of the car against UAV threats within a radius of up to 35 m.

Keywords: 3D object detection, 360° LiDAR scans, UAV detection, UAV tracking, scanline analysis

1. INTRODUCTION

The worldwide availability of low-cost UAVs that are easy to operate leads to rising problems, ranging from misleading toys up to abusive use of UAVs for spying or other hostile activities. Especially with regard to sensible areas like airports, company premises or military facilities, options for the detection, tracking and monitoring of UAVs are needed.

Not only the small size of UAVs renders their detection and tracking a complicated task. Their high acceleration capacity, their high top speed and their great maneuverability in all three dimensions make it hard to track the UAVs or to predict their paths reliably. Nevertheless, most of the known standard surveillance techniques can be applied for UAV detection:

- There are various approaches with cameras in the visible [1] [2] and the SWIR [3] spectra. For all camera-based algorithms, the main challenge is the separation of the object from the background. Furthermore, the detection results are mainly dependent on the quality of the images, e.g., the resolution and the focus on the object.
- Another well-proven technique for the detection of (flying) objects is the use of radar sensors. Noetel et al. [4] describe two types of millimeter wave radars for the detection and tracking of small UAVs. The UAV detection with radar is limited mainly by the low radar cross-section of most UAVs.
- The detection of UAVs with acoustical sensors is described by Christnacher et al. in [5]. Based on acoustic antenna arrays, the acoustic signatures of flying UAVs are measured continuously. With this hardware setup, a wide range of UAV sounds (up to 6.8 kHz) can be detected and tracked.

¹ marcus.hammer@iosb.fraunhofer.de; phone +49 7243 992-303; fax +49 7243 992-299; www.iosb.fraunhofer.de

- The use of active imaging in the form of gated viewing for UAV detection and tracking is presented by Christnacher et al. in [5]. The main advantage of gated viewing in contrast to the imaging with CCD cameras is the option to set the gate around the object and to suppress the foreground and the background. For this purpose, the distance to the UAV has to be known initially.
- A multimodal sensing approach was investigated by application of a multi-sensor network consisting of RADAR and acoustic signature detection and tracking as well as active and passive optical identification [6] [7] [8] [9].
- Further, first investigations consider the application of scanning LiDAR (light detection and ranging) systems [8] [10].

3D point clouds acquired by LiDAR sensors have proven to be a good basis for object detection, e.g., for persons [11], cars [12] or ships [13]. Today's available scanning LiDAR systems represent a compromise between acceptable resolution, realizable refresh rate and field of view (FOV). The sparse resolution of most LiDAR sensors seems to make them rather unsuitable for UAV detection. On the other hand, LiDAR-based detection methods show many advantages: the separation of the object from fore- or background is comparatively easy, the exact 3D position of the object is known instantaneously after its detection, and the sensor is not dependent on daylight conditions.

In this paper, we assess the potential of different LiDAR sensors for the detection of UAVs and investigate the detection performance relative to the detection range. For the assessment of the visibility of different UAV types, an example of experimental LRCS investigation is shown.

2. DATASET

For our experiments we used data which we acquired with the measurement vehicle MODISSA [14] during a joint field trial in cooperation with the Institut Franco-Allemand de Recherches de Saint-Louis (ISL) and the Fraunhofer Institute for High Frequency Physics and Radar Techniques FHR [9].

2.1 Sensor platform MODISSA

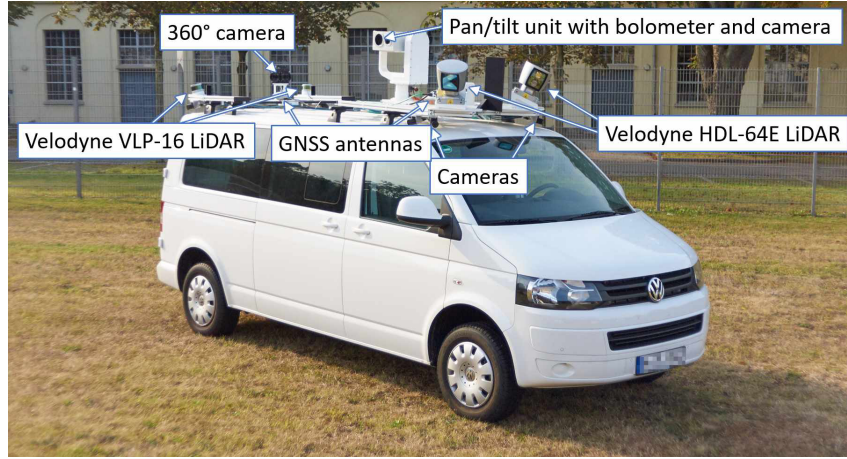


Figure 1: The sensor platform MODISSA is equipped with several sensors including four 360° LiDAR scanners.

The vehicle shown in Figure 1 is equipped with several scanning LiDAR sensors, various cameras for omnidirectional monitoring, an EO- and a SWIR camera on a pan-tilt head and an inertial measurement unit (IMU) and two GNSS (GPS, GLONASS) receivers. We used the two LiDAR sensors Velodyne HDL-64E mounted on the roof in the front of the vehicle in combination with the two LiDAR sensors Velodyne VLP-16 PUCK mounted on the roof in the back of the car. Each HDL-64E is capable of performing 1.3 million measurements per second in a range up to 120 meters. Its vertical FOV is 26.9°, divided into 64 scanlines resulting in a vertical resolution of 0.4°. Due to the rotating sensor head, the horizontal field of view covers 360° with a resolution of about 0.17° at a typical rotation frequency of 10 Hz. This means that every point cloud of a single 360° scan could consist of approximately 130 000 measurements. However, since not every emitted laser pulse results in the detection of a returning echo (e.g., measurements directed to the sky or water surfaces), the resulting point clouds are usually smaller. The smaller VLP-16 has a vertical FOV of 30° generated by 16

scanlines, leading to a vertical resolution of 2° . At a rotation frequency of 10 Hz, the horizontal resolution is about 0.2° and a single 360° scan could consist of up to 30000 measurements (3D points). The recording of the LiDAR measurements is time-synchronized and the geometric constellation of the four sensors is known, so the four individual point clouds can easily be merged together in a common coordinate system.

The two HDL-64E sensors are mounted to the sensor carrier with a tilt of 25° downwards and an angle of 45° outwards (cf. Figure 1), the VLP-16 are mounted to it with a tilt of 15° downwards and 45° outwards. This special configuration leads to an enlarged FOV in upwards directions (e.g., towards the facades of buildings). Otherwise, if an HDL-64E is horizontally mounted as intended by the manufacturer for applications like autonomous driving, its FOV would cover $+2^\circ$ to -25° in elevation, which would be inappropriate for UAV detection. With our setup, elevation angles up to $+27^\circ$ are realized, at least in parts of the surrounding.

2.2 Field trial

A field trial took place on a testing ground near Baldersheim (France). Its main goal was the acquisition of realistic sensor data in order to assess the capabilities of different sensor technologies for the detection, tracking and identification of small unmanned aerial vehicles (mini/micro UAVs) flying at low altitude. An additional aspect of these activities was the investigation of a sensor network, comprising of a small radar system, distributed acoustic antennas, passive/active EO/IR imaging and static as well as vehicle-mounted LIDAR sensors [9]. The sensor vehicle MODISSA was used both stationary and moving. Within this setup, different types of small UAVs (see Figure 2) were used for different scenarios like an ascending/descending UAV, an approaching UAV, a UAV that flies attacks, UAV in high altitude patrol, UAV in fast flyby and multiple UAVs in various maneuvers.



Figure 2: Different mini/micro UAVs that were used during the field trial (a): DJI Phantom 3, (b): Parrot Bebop 2, (c): Parrot Disco, (d): DJI MAVIC Pro.

2.3 Laser RADAR Cross-Section measurements

The quality of object detection with LiDAR sensors is not only dependent on the sensor resolution. The reflectivity of the object is at least equally important. Because UAVs are small, have a complex structure and are built of various materials, we wanted to quantify their reflectivity and therefore the visibility for LiDAR sensors. For this purpose, we examined the Laser RADAR Cross-Section.

For a LiDAR system, the received number of photons or the intensity of the impinging photon flux from a resolved target surface is defined by the LiDAR equation [15] in (1). Here, P_T is the transmitted optical power, σ is the laser radar cross section (LRCS), A_{illum} and A_{rec} are the illuminated area and the receiver surface, respectively, and R is the range. Furthermore, η_{atm} and η_{sys} describe the optical transmission efficiency of the atmosphere and the optical system.

$$P_R = P_T * \frac{\sigma}{A_{illum}} * \frac{A_{rec}}{\pi R^2} * \eta_{atm}^2 * \eta_{sys} \quad (1)$$

The LRCS σ describes a relative target dimension and has been defined by Wyman [16] as the ratio of the impinging optical irradiance H (W per unit area) and the total scattered power P_S per steradian $\sigma = P_S / H$. In 1992, Osche et al. [17] have established a method to determine the LRCS from high resolution point clouds. Later, Laurenzis et al. [18] [19] have adapted this method to the use of active imaging data and images from computational rendering.

In Figure 3, an example of experimental LRCS investigation from active imaging data is illustrated. The experiments were carried out in a low light level tunnel at the French-german Research Institute using a shortwave infrared (SWIR) active imaging system, as described by Christnacher et al. [5].

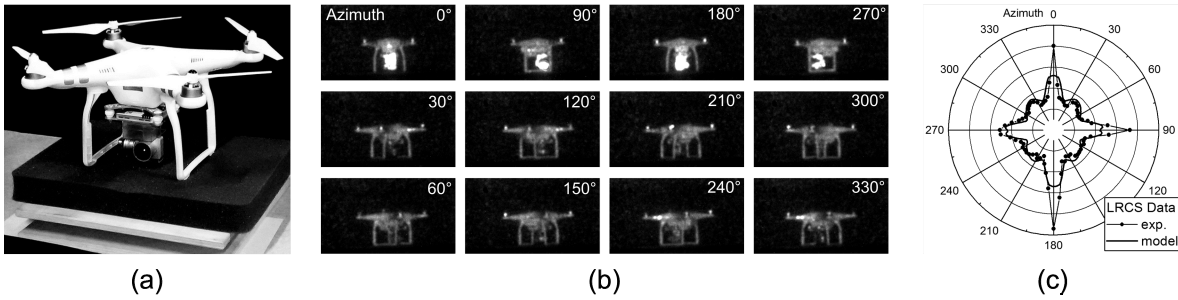


Figure 3: LRCS of an actual UAV were determined by active imaging in a low light level facility at ISL and compared to theoretical models: (a) UAV on rotary stage, (b) images of the UAV at different rotation angles and (c) comparison of experimental LRCS data and LRCS model.

In Figure 3 (a), the image illustrates the mounting of the UAV on a rotary stage at a range of 40 m in front of the SWIR gated viewing system. In (b) SWIR gated viewing images of the UAV at different rotation angles are shown. From these images, the LRCS of the UAV could be derived by integration of all intensity values. In Figure 3 (c), the experimental results are compared to a theoretical model.

The experimental data points (filled circles with solid line) were calibrated to a diffuse white. The UAV shows a nearly isotropic cross section of $\text{LRCS} = 0.015 \text{ m}^2$ in most directions. Some significant high LRCS peaks occur at angles of 0 deg; 90 deg; 180 deg; and 270 deg, where specular reflections of light occur. Here, a maximum LRCS of 0.047 m^2 can be observed which is three times higher than the LRCS at other rotation angles.

3. METHODOLOGY

The proposed object detection and tracking algorithm takes advantage of the dense, ordered structure of the point clouds corresponding to single 360° rotations of the laser scanner (organized clouds). In the following, we call that a single *scan* or *frame*, consisting of n rows or scanlines ($n=64$ for the HDL-64E, $n=16$ for the VLP-16) and m columns (m depending on the pulse repetition rate and the rotation frequency of the scanner head). With the Velodyne sensors, single frames are generated such that for every emitted laser pulse a data value is recorded, even if it is NaN since no actual measurement was possible (too far, low reflectance etc.). Due to this ordered data structure, for each point the range value of its neighboring points within the same scanline can easily be determined, similar to a range image.

3.1 Segmentation of single 360° scans

As we have shown in an earlier work [20] and as it is known from literature [21], a fast geometric 3D segmentation is possible if the 3D data are given as organized point clouds like it is described above, i.e., if the range of neighboring pixels in rows of the range image is known. At first, this requires a 2D segmentation where neighboring points of a row are clustered as long as no changes in range exceeding a given threshold are found. All line segments (that means at least two neighboring points) with a width less than the maximum width of a target object (we assumed up to 1.2 m for the examined small UAVs, see Figure 2) are further examined as possible target-related 2D clusters. Due to the high variety (a 2D cluster could contain between two and over 200 points), a high number of 2D clusters is detected for each sensor, most of them being artefacts of rough ground in higher distance.

3.2 Merging of 3D point clouds and 3D clustering

The four time-synchronized LiDAR sensors of MODISSA are mounted to the sensor carrier with a fixed, known relative orientation, such that the individual point clouds can be transferred to a common coordinate system. Therefore, it is easy to merge the 2D cluster we get from the individual segmentation runs into one large cluster set. All these 2D clusters are further merged to 3D clusters if they overlap horizontally and do not exceed a maximum vertical distance. 3D clusters with an overall width in x-y direction or a height (z dimension) wider than the maximum dimensions of a UAV are rejected. The number of 3D clusters typically varies between a few and more than several hundred potential objects per frame. Assuming that a UAV has to keep a minimum distance to the scene (walls, trees or the ground), we find 3D clusters that are isolated in the point cloud, i.e., 3D clusters that have no or only very few other points in their direct neighborhood. This detection of isolated clusters is done with an occupancy grid which is set up with all points of all four sensors and a grid size of 0.5 m. As a result, the number of potential UAV objects can typically be reduced from several hundred to less than twenty for each frame.

Because of the small LRCS of the UAVs (see Section 2.3) and the limited resolution of the LiDAR scanner, the number of points per UAV is low, even on short distances. Due to this fact, a further geometric analysis of the point cloud objects (the remaining 3D clusters) is not very promising. A better approach for a further classification of the object (UAV/non-UAV) is the analysis of its movement. This requires a tracking of the 3D clusters.

3.3 Tracking of 3D clusters

We record the continuous data stream of each Velodyne LiDAR sensor in such a way that it is subdivided into single 360° scans (frames). An object detected in the last frame should occur in the current frame at a position near its last position or the extrapolated next position. In order to find such corresponding objects, a track list is set up with all detected objects of the first frame. For all subsequent frames, the coordinates of all detected 3D objects are compared with the objects in the track list. Each new object is assigned to that object of the track list with the minimum distance. If there is no such object in the track list with a distance below a threshold, the new object is set as a new track. Regardless of a current observation, for each object in the track list a prediction of its further movement is calculated using a Kalman filter. Several features like the current speed and the overall motion can be calculated for each object in the track list. For a classification as UAV, an object has to be detected at least three times consecutively, the current velocity and acceleration has to be in a realistic range and there has to be an overall movement of at least 0.5 m. This overall movement eliminates objects like flags or parts of trees which show an oscillating movement with acceptable velocity and acceleration. Objects without any movement can be classified as non-UAV. The prediction of the movement makes it possible to continue the track of an object even after some missing detections if the object keeps its last trajectory constant.

4. EXPERIMENTAL RESULTS

4.1 Field Trial

During the field trial, we recorded over 1 hour of data of eight different scenarios, of which 57 % are supplemented with ground truth data, provided by GPS-receivers attached or belonging to the UAVs. Due to the limited FOV of the LiDAR sensors, only few scans contain a UAV object. A UAV was detected in 4704 of 39476 frames (12 %). For a quantitative evaluation of our methods (precision and recall), only the scenarios with ground truth information are considered. Overall, in 22476 frames 2339 UAVs should have been detectable, meaning that the UAV was in the FOV and in a range of less than 50 m.

4.2 Detection rate

It is hard to give precise numbers like precision and recall for the detection rate, because such calculations would require accurate ground truth information. The ground truth recorded for the UAV's trajectories is derived from their onboard GPS sensor, but the accuracy of that data is limited due to the low update rate of the GPS readings, given the high speed of the UAVs. On the other hand, the overall FOV of the LiDAR sensors in our system is quite complex, due to the different tilt angles of the sensors (see Section 2.1). In detail, the height of the UAV is crucial for its detectability. The height values measured by GPS are generally more blurred than the horizontal values and while scanning 360° horizontally, the vertical FOV of the LiDAR sensors is strictly limited. Furthermore, due to the number of sensors on our sensor platform MODISSA, the FOV of individual sensors can be restricted by other sensors in the line of sight. Therefore, it is hard to decide if a UAV (with blurred GPS height) should have been detectable by a LiDAR sensor.

Although the ground truth information may be imprecise that way, we calculated a detection rate or recall (true positives (TP) divided by the sum of true positives and false negatives (FN)) as well as the precision (TP divided by the sum of TP and false positives (FP)) for our system of four LiDAR sensors. In this analysis, we considered only those measurements that had supplementary ground truth data available. In three scenarios, 2339 UAVs should have been visible in the FOV of the sensors, 1248 of them were detected correctly (TP). 1091 UAVs were probably visible in the FOV but were not detected (FN). The recall is estimated to 53.3 %, which should be seen as a lower bound, given the imperfect ground truth information. To reduce the amount of objects erroneously classified as UAVs (FP), a number of optimizations in the classification step were introduced, especially the tracking algorithm with speed and acceleration evaluation. As a result only 47 FP were found and the precision can be estimated to 95.6 %.

4.3 Sensor suitability

The above numbers were obtained using all four available LiDAR sensors. But it has to be considered that the quality of the data of the two sensor types differ in large numbers. The smaller VLP-16 is comparatively inexpensive and easy to

use, but its vertical resolution is about five times lower than that of the HDL-64. In 12.5 m distance, the gap between two consecutive scanlines of the VLP-16 is 0.43 m (HDL-64: 0.09 m, see Figure 4 (a) and (b) for typical scan patterns of the two sensors in 12.5 m distance), leading to a high probability of missing the UAV. This results in remarkably different recall numbers for the two sensor systems. 1843 UAVs have been in the FOV of the two HDL-64 of which 1151 were detected, resulting in a recall of 62.5 %. In contrast only 97 UAVs were detected by the two VLP-16 while 496 UAVs should have been visible, resulting in a recall of 19.6 %. This example illustrates that even in the low distance of 12.5 m, the VLP-16 hits the object only by chance. The histogram of detected UAVs of the two sensor types (in Figure 4 (c)) shows that the VLP-16 detected UAVs only in low ranges. This leads to the conclusion that 360° scanning LiDAR systems with a low (vertical) resolution are not well suited for UAV detection in useful distances.

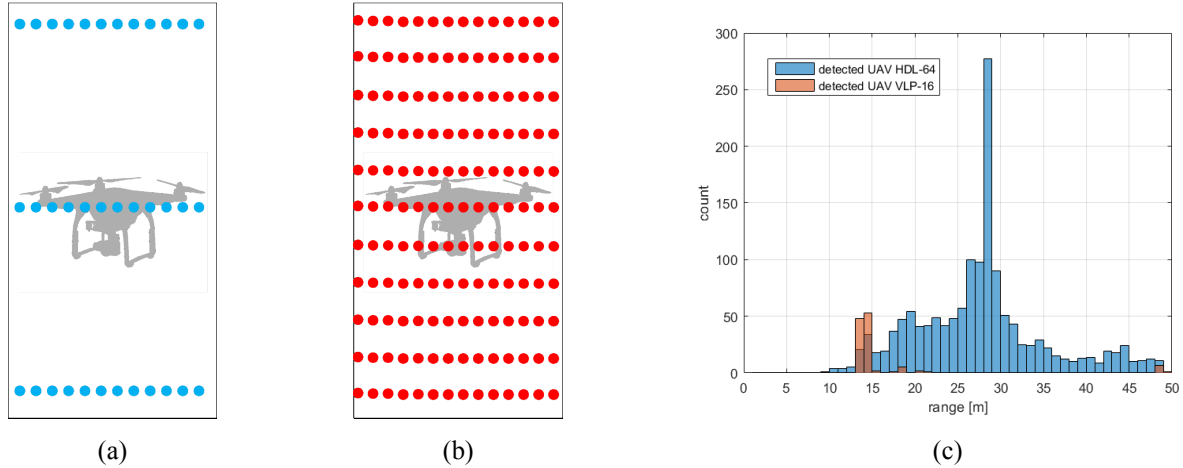


Figure 4: Typical LiDAR scan pattern in 12.5 m distance of (a) VLP-16 (blue) and (b) HDL-64 (red), (c) histogram of detected UAVs, blue HDL-64, orange VLP-16

4.4 Detection range

The maximum range in which a UAV can be detected is a crucial parameter for the use of a panoramic scanning LiDAR system. The Velodyne sensors are optimized for applications like autonomous driving, not for long-range UAV detection. The maximum range of the HDL-64E is specified with 120 m for a target with 80 % reflectivity. Due to the small LRCS of most UAVs (see Section 2.3), it is to be expected that the maximum range for UAV detection is much shorter, even under good other circumstances.

Because the detection performance of the VLP-16 is hampered by its vertical resolution (as discussed in Section 4.3), the following analysis is performed only with the datasets of the HDL-64. We divided the 1843 UAVs in the FOV into eight range classes, each five meters wide, and calculated the recall for each class (see Figure 5).

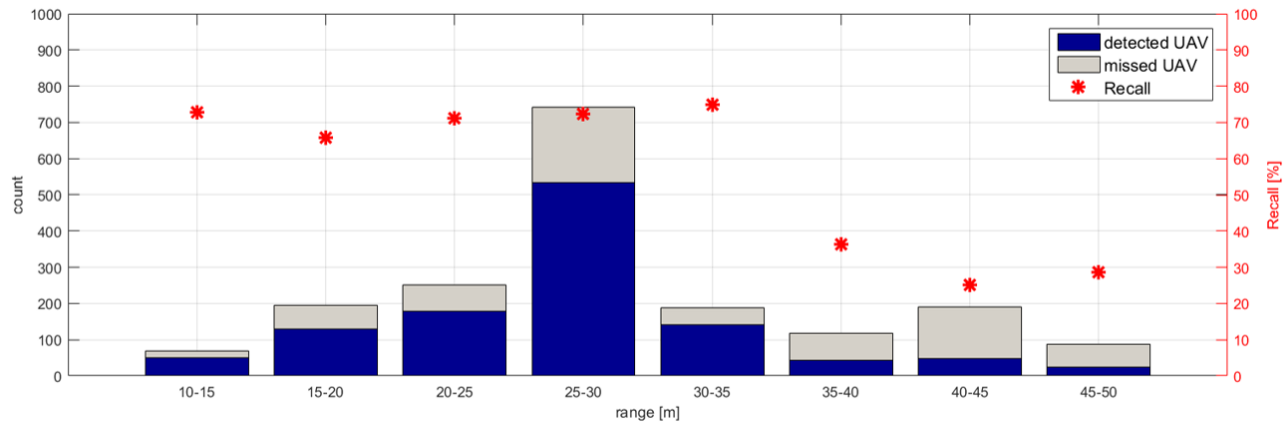


Figure 5: UAVs detected and missed by the HDL-64 in range classes (distance by ground truth) and related recall numbers

The absolute number of UAVs in each class is mainly related with the movement of the UAVs, which were flying by more often in the 25 m to 30 m range. On the other hand, the recall is independent of the absolute number and it is quite high around 70 % for ranges below 35 m and drops to numbers around 30 % for ranges above.

If we have a look onto the theoretical scan patterns in each range class (Figure 6), it can be noted that the decline of the recall above 35 m comes along with the vertical distance between two scanlines getting significantly larger than the height of the target. The decreasing point density in horizontal direction may reduce the recall as well, but it seems as if the vertical resolution of the sensor is crucial.

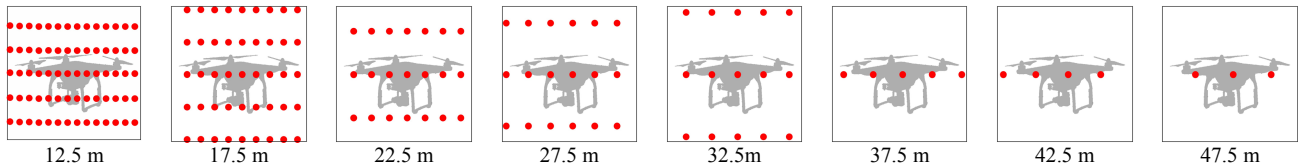


Figure 6: Theoretical scan patterns (scan point resolution) in different distances for the HDL-64 with a target outline

The self-imposed detection limit of 50 m was chosen such that a minimum of two points should result from the target if the target is hit by the horizontal scanline. Considering the range-related recall values mentioned above, a maximum detection limit of 35 m seems to be more suitable for an acceptable detection rate. Using these two constraints, only considering the two HDL-64 and a maximum detection range of 35 m, we are able to detect 894 of 1259 UAVs in the FOV. This results in a recall of 71.0 % which is quite high, having in mind the problematic ground truth situation.

4.5 Path prediction

As mentioned in Section 3.3, we use a Kalman Filter for the prediction of the next position of each tracked object. Thus, we have an estimated position of the UAV even when the sensor is temporarily not able to retrieve a signal of it. If we use these virtual UAV positions, we get recall values as shown in Figure 7.

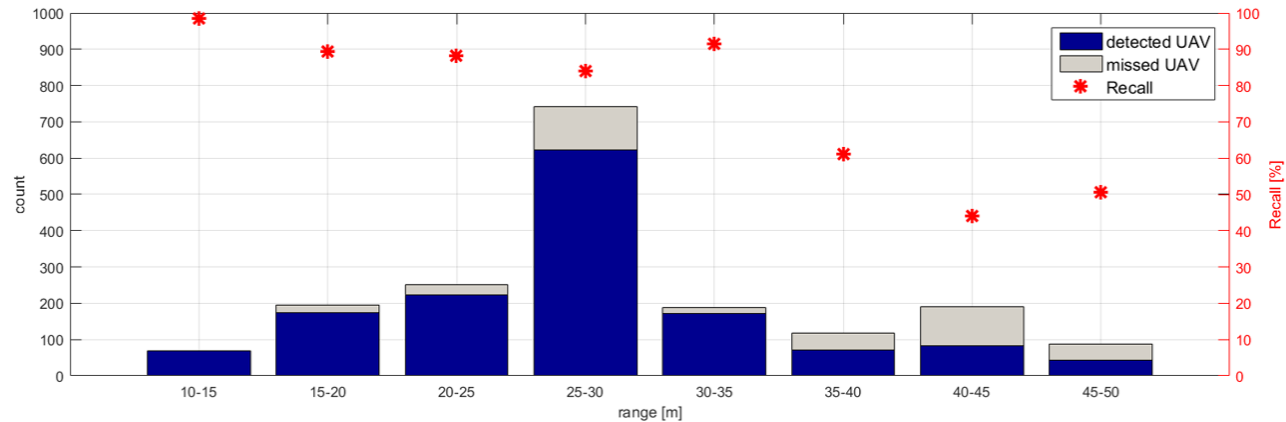


Figure 7: UAVs detected and missed by the HDL-64 (including extrapolated positions of UAVs) in range classes (distance by ground truth) and related recall numbers

For all range classes the number of undetected UAVs is reduced and the recall is increased. Nevertheless, the significant drop in recall above 35 m is still present. With these optimized parameters (distance < 35 m, only HDL-64 and path prediction), 1261 of 1447 UAVs are detected resulting in a recall of 87.1 %.

5. CONCLUSIONS AND FUTURE WORK

In this paper, we investigated the detection performance relative to the detection range of two different 360° LiDAR systems. We have shown that it is possible to detect UAVs with a high probability, as long as the UAV is in the FOV of the sensor and the distance between sensor and UAV is not too big. A remarkable finding was the reduction of the detection rate for distances above 35 m, which can be traced back to the low point density on targets. In addition, the gap between the scanlines allows UAVs to remain undetected in these distances. It can be noted that the smaller VLP-16 sensor is not very well suited for UAV detection in ranges above 10 m. On the other hand, the HDL-64 shows good results for distances up to 35 m and a basic usability for distances up to 50 m. Due to the detection by tracking approach, a detection

can only take place after at least three observations, which leads to at least two objects being unclassified at the beginning of the corresponding track. The complex FOV of the LiDAR sensors on our sensor vehicle MODISSA can lead to missed UAV detections due to occlusions by other hardware on the sensor carrier, but it seems as if this problem could mainly be solved using the predicted positions of the UAVs from the track list.

The analysis of the range dependent recall suggests that the maximum point distance on the target should not exceed the minimum target dimension, i.e., in case of the UAVs, a height of 25 cm. For the Velodyne HDL-64E, this critical point gap is reached at 35 m target distance. With this knowledge, we can calculate the sensor specification for a LIDAR based UAV detection in 50 m distance (sensor resolution < 0.28°) or even for 100 m distance (sensor resolution < 0.14°). However, even with a LiDAR sensor with such a high resolution, the detection rate most probably will decrease due to the low LRCS and therefore low backscattered signal of the UAV.

The major advantage of LiDAR-based UAV detection is the automatically measured 3D coordinate of the UAV. Especially for applications like close-range facility protection and for countermeasures, an accurate trajectory of the UAV is needed. Besides that, LiDAR is robust against changes in illumination and environmental conditions. Although a set of different mini/micro UAVs was utilized in the field trial, the presented results do not pay attention to the differences between the UAV types. For one UAV type, the LRCS was experimentally investigated. The impact of the LRCS of different UAVs onto the detection rate should be further examined. The results presented in this paper should be validated with another set of data. The tracking and detection algorithm should also be tested in scenarios with multiple UAVs. Particular attention should be given to an accurate ground truth of the UAV path.

6. REFERENCES

- [1] Ganti, S. R., Kim, Y., "Implementation of detection and tracking mechanism for small UAS," International Conference on Unmanned Aircraft Systems (ICUAS), Arlington, VA USA, (2016).
- [2] Hu, S., Goldman, G. H., Borel-Donohue, C. C., "Detection of unmanned aerial vehicles using a visible camera system," Applied Optics Research, Vol. 56, No. 3, (2017).
- [3] Müller, T., "Robust drone detection for day/night counter-UAV with static VIS and SWIR cameras," Proc. SPIE 10190, Ground/Air Multisensor Interoperability, Integration, and Networking for Persistent ISR VIII, (2017).
- [4] Noetel, D., Johannes, W., Caris, M., Hommes, A., Stanko, S., "Detection of MAVs (Micro Aerial Vehicles) based on millimeter wave radar," Proc. SPIE 9993, Millimetre Wave and Terahertz Sensors and Technology IX, 999308, (2016).
- [5] Christnacher, F., Hengy, S., Laurenzis, M., Matwyschuk, A., Naz, P., Schertzer, S., Schmitt, G., "Optical and acoustical UAV detection," Proc. SPIE 9988, Electro-Optical Remote Sensing X, 99880B, (2016).
- [6] Hommes, A., Shoykhetbrod, A., Noetel, D., Stanko, S., Laurenzis, M., Hengy, S., and Christnacher, F., "Detection of acoustic, electro-optical and radar signatures of small unmanned aerial vehicles," in [Target and Background Signatures II], 9997, 999701, International Society for Optics and Photonics (2016).
- [7] Hengy, S., Laurenzis, M., Schertzer, S., Hommes, A., Kloeppe, F., Shoykhetbrod, A., Geibig, T., Johannes, W., Rassy, O., and Christnacher, F., "Multimodal UAV detection: study of various intrusion scenarios," in [Electro-Optical Remote Sensing XI], 10434, 104340P, International Society for Optics and Photonics (2017).
- [8] Laurenzis, M., Hengy, S., Hommes, A., Kloeppe, F., Shoykhetbrod, A., Geibig, T., Johannes, W., Naz, P., and Christnacher, F., "Multi-sensor field trials for detection and tracking of multiple small unmanned aerial vehicles flying at low altitude," in [Signal Processing, Sensor/Information Fusion, and Target Recognition XXVI], 10200, 102001A, International Society for Optics and Photonics (2017).
- [9] Laurenzis, M., Hengy, S., Hammer, M., Hommes, A., Johannes, W., Giovanneschi, F., Rassy, O., Bacher, E., Schertzer, S., and Poyet, J.-M., "An adaptive sensing approach for the detection of small UAV: first investigation of static sensor network and moving sensor platform," in [Signal Processing, Sensor/Information Fusion, and Target Recognition XXVII], 10646, 106460S, International Society for Optics and Photonics (2018).
- [10] Hammer, M., Hebel, M., Borgmann, B., Laurenzis, M., and Arens, M., "Potential of LiDAR sensors for the detection of UAVs," in [Laser Radar Technology and Applications XXIII], 10636, 1063605, International Society for Optics and Photonics (2018).

- [11] Spinello, L., Luber, M., Arras, K. O., "Tracking people in 3D using a bottom-up top-down detector," IEEE Int. Conf. on Robotics and Automation (ICRA), (2011).
- [12] Li, B., Zhang, T., Xia, T., "Vehicle detection from 3D LiDAR using fully convolutional network," In Robotics: Science and Systems, (2014).
- [13] Armbruster, W. Hammer, M., "Segmentation, classification, and pose estimation of maritime targets in flash-ladar imagery," SPIE Proceedings, Volume 8542, Signal and Image Processing I, (2012).
- [14] <https://www.iosb.fraunhofer.de/servlet/is/42840/>
- [15] McManamon, P., "Review of ladar: a historic, yet emerging, sensor technology with rich phenomenology," Optical Engineering 51(6), 060901 (2012).
- [16] Wyman, P. W., "Definition of laser radar cross section," Applied Optics 7(1), 207-207 (1968).
- [17] Osche, G., Seeber, K., Lok, Y., and Young, D., "Laser radar cross-section estimation from high-resolution image data," Applied optics 31(14), 2452-2460 (1992).
- [18] Laurenzis, M., Bacher, E., Christnacher F., "Experimental and rendering-based investigation of laser radar cross-sections of small unmanned aerial vehicles," Optical Engineering, 56 (12), 124106, (2017).
- [19] Laurenzis, M., Bacher, E., and Christnacher, F., "Measuring laser reflection cross-sections of small unmanned aerial vehicles for laser detection, ranging and tracking," in [Laser Radar Technology and Applications XXII], 10191, 101910D, International Society for Optics and Photonics (2017).
- [20] Hammer, M., Hebel, M., Arens, M., "Person detection and tracking with a 360° LiDAR system," Proc. SPIE 10434, 104340L, (2017).
- [21] Jiang, X., Bunke, H., "Fast Segmentation of Range Images into Planar Regions by Scan Line Grouping," Machine Vision and Applications 7 (2), pp. 115-122, (1994).